Electronic Supplementary Material (ESI) for Molecular Systems Design & Engineering.
This journal is © The Royal Society of Chemistry 2016

Electronic Supplementary Information for

Robust Control over Morphologies and Grain Interfaces of Three-Dimensional Well-Ordered Superstructures Programmed by Hybrid Topographical-Chemical Templates

Zhinan Cong, Liangshun Zhang, Liquan Wang and Jiaping Lin**

Shanghai Key Laboratory of Advanced Polymeric Materials, State Key Laboratory of Bioreactor Engineering, Key Laboratory for Ultrafine Materials of Ministry of Education, School of Materials Science and Engineering, East China University of Science and Technology, Shanghai 200237, China

*Corresponding Author E-mail: zhangls@ecust.edu.cn; jlin@ecust.edu.cn

Contents

Part A: Model of Block Copolymers in Templates

To explore the complex 3D structures of block copolymers in the templates, the model developed here is based on the standard Hamiltonian used in the polymeric field-theoretic approach with mean-field approximation.[S1] The systems with volume V consist of n monodisperse AB diblock copolymers confined between two solid surfaces, which are schematically illustrated in Figure 1. The block copolymers have a length $N=N_A+N_B$ and ideal gyration radius R_g. The volume fraction of A blocks is given by $f_A=N_A/N$. In the cases of chemical templates, both the top and bottom surfaces contain the chemical stripes with periodicity L_s and width W_s, which are orthogonal to each other (Figure 1a). In the cases of hybrid templates, the bottom chemical stripes are replaced by a period arrangement of posts with periodicities L_y and L_z in the y and z directions (Figure 1b).

The effective Hamiltonian H for the AB diblock copolymers in the templates has the following form

$$\frac{H\left[W_+,W_-,W_{ext}^{A},W_{ext}^{B}\right]}{C} = \int_{\bar{V}} dr\left[\frac{1}{\chi_{AB}N}W_-^2(r) - \frac{2\zeta N}{\chi_{AB}N+2\zeta N}iW_+(r) - \frac{1}{\chi_{AB}N+2\zeta N}\left(iW_+(r)\right)^2 + \frac{\lambda(r)}{\chi_{AB}N}W_-(r)\right] - \bar{V}\,lnQ\left[W_+,W_-,W_{ext}^{A},W_{ext}^{B}\right]$$

In this expression, C and $\bar{V}$ are the dimensionless concentration of chains and volume, respectively. The stiffness parameter ζN controls the strength of density fluctuations in the Helfand form. W_+ is a pressure field that couples to total density variations, and W_- is an exchange field conjugated to the density difference between the A and B segments. Q is the normalized single-chain partition function for a diblock copolymer chain. While the above field theory of polymeric fluids is formally exact, we restrict our simulations to the mean-field limits named self-consistent field theory (SCFT), which is given by $\left.\frac{\delta H}{\delta iW_+}\right|_{W_\pm^*}=0$ and $\left.\frac{\delta H}{\delta W_-}\right|_{W_\pm^*}=0$. More details about the numerical methods can refer to our previous work.[S2]

In our model, the topographical posts are introduced by additional spatially varying local external fields W_{ext}^{A} and W_{ext}^{B} with a hyperbolic tangent form [S3]

$$W_{ext}^{I} = W_0\left(1-\tanh\left(\frac{\sqrt{y^2+z^2}-R}{\xi^I}\right)\right)\left(1-\tanh\left(\frac{x-\Delta}{\xi^I}\right)\right) \text{ (I=A, B)}$$

Here, R and Δ are the radius and height of posts, respectively. The strength W_0 of external fields is fixed at W_0=40.0 to prevent the polymers from penetrating into the posts. The steepness ξ_A and ξ_B of the potential change at the well edge for the A and B blocks are set as $0.10R_g$ and $0.20R_g$, respectively. The small value of W_{ext}^{A} at the well edge promotes the weakly preferential wetting of the A blocks to the posts.

The interactions between the polymers and the chemically patterned surfaces are represented by [S4]

$$\lambda(r) \equiv \lambda(x,y,z) = -\lambda^t N f_t(y,z) exp\left(-(x-H)^2/2\epsilon^2\right) - \lambda^b N f_b(y,z) exp\left(-x^2/2\epsilon^2\right)$$

which decays over a short distance ε. $\lambda^t N$ ($\lambda^b N$) determines the strength of interactions between the blocks and the top (bottom) surfaces. For simplicity, we assume that the attraction for the A (B) blocks is equal in magnitude to the repulsion for the B (A) blocks for the chemically patterned surfaces. The functions f_b and f_t describe the chemical stripes as functions of the lateral coordinates y and z on the bottom and top surfaces, respectively. There values are 1 in the B-attractive stripes and -1 in the A-attractive stripes. To achieve the vertical lamellae registered by the chemical templates, the stripes (background areas) are preferential for the B (A) blocks, *i.e.*, the interactions between the top (bottom) surfaces and blocks $\lambda^t N$ ($\lambda^b N$)=10.0. In the hybrid templates, the chemical selectivity of top surfaces is the same as that of chemical templates. To produce the vertical lamellae programmed by the posts, the bottom surfaces are assumed to be neutral, *i.e.*, $\lambda^b N$ =0.0.

We perform the simulations in the large cells with lattice size 48×192×192. To overcome the computational task, the GPGPU (General-Purpose Graphics Processing Unit) using the NVIDIA® CUDA™ architecture is adopted to accelerate the numerical solutions of SCFT

equations of polymeric fluids. The initial configurations of the simulations are homogenous states. To reduce the defects of patterns and increase the correlation length of domain order, a slowly thermal annealing process is applied.[S5] It should be pointed out that the large-size systems of block copolymers guided by the chemical stripes usually trap into the metastable states with poorly order in the cases of film thickness $H \geq 5.0R_g$. To pursue the well-ordered architectures formed in the chemical templates, we perform the small-cell simulations with lattice size 48×48×48, where the defective structures could "evolve" into the highly ordered structures.

It should be mentioned that influence of box sizes on the directed self-assembly nanostructures of block copolymers is complicated due to the commensurability conditions between the natural periodicity of block copolymer domains and the dimensions of topographical posts or chemical stripes.[S6] As the post periodicities and stripe width satisfy the commensurability conditions, the directed self-assembly behaviors of block copolymers in the large boxes are very similar with those of small boxes. This is demonstrated by the 3D superstructures obtained from the simulations with box size in the range of $6.5R_g \times 18.0R_g \times 18.0R_g$~$6.5R_g \times 72.0R_g \times 72.0R_g$ (Figures S1a~S1c). It should be pointed out that the parameter settings of templates in Figures 2, 3 and 5 satisfy the commensurability conditions. As the periodicities of posts and stripes are largely deviated from the commensurability conditions, another scenario is observed. As shown in Figure S1d, the block copolymers in the small boxes self-assemble into the ordered structures with high internal stress. However, the well-ordered nanostructures with controlled orientations cannot be achieved in the large-cell simulations of SCFT (Figures S1e and S1f).

To quantitatively measure the positions of grain interfaces, we introduce position parameters m to describe the difference (ϕ_B-ϕ_A) of local volume fractions between the B and A blocks in unit cells, which are defined as $m \equiv \frac{1}{2V_0}\int_{V_0} dr\,(s_b - s_t)(\phi_B(r) - \phi_A(r))$.[S7] Here, V_0 is the

volume of unit cells having different domains on the top and bottom surfaces as shown in Figure 2b. The functions s_b and s_t describe the B-rich domains as functions of the lateral coordinates y and z on the bottom and top surfaces, respectively. Their values are 1 in the B-rich domains and -1 in the A-rich domains. It is obvious that the grain interfaces located at the center of cells V_0 will result in m=0. As the position parameters m are larger than zero, the interfaces will move towards the top surfaces. Conversely, the interfaces will be located in the bottom part of films for m<0. Thus, the position parameters m could be utilized to characterize the positions of grain interfaces in the 3D ordered structures.

To capture the statistical behaviors of position parameters of 3D ordered structures in the unit cells, 240 unit cells (1 structure obtained from the large-cell simulations, 240 unit cells/structure) are analyzed to obtain the data of a histogram. To construct the histograms with error bars (Figure 3), 24 independent realizations with different random seeds are conducted, *i.e.*, the sample size N=24. The error bars represent the standard deviations from the mean values, which are defined as $SD(p(m)) \equiv \sqrt{\sum_{i=1}^{N} \left(p^i(m) - p(m)\right)^2 \Big/ (N-1)}$ with mean values $p(m) \equiv \sum_{i=1}^{N} p^i(m) \Big/ N$. In the cases of chemical templates, the same numbers of unit cells (30 structures obtained from the small cell simulations, 8 unit cells/structure) and the same size of samples (N=24) are used to generate the histograms of position parameters (Figure 2). It should be mentioned that the directed self-assembly behaviors of block copolymers are very similar in the cases of the large- and small-cell simulations for the thin films.

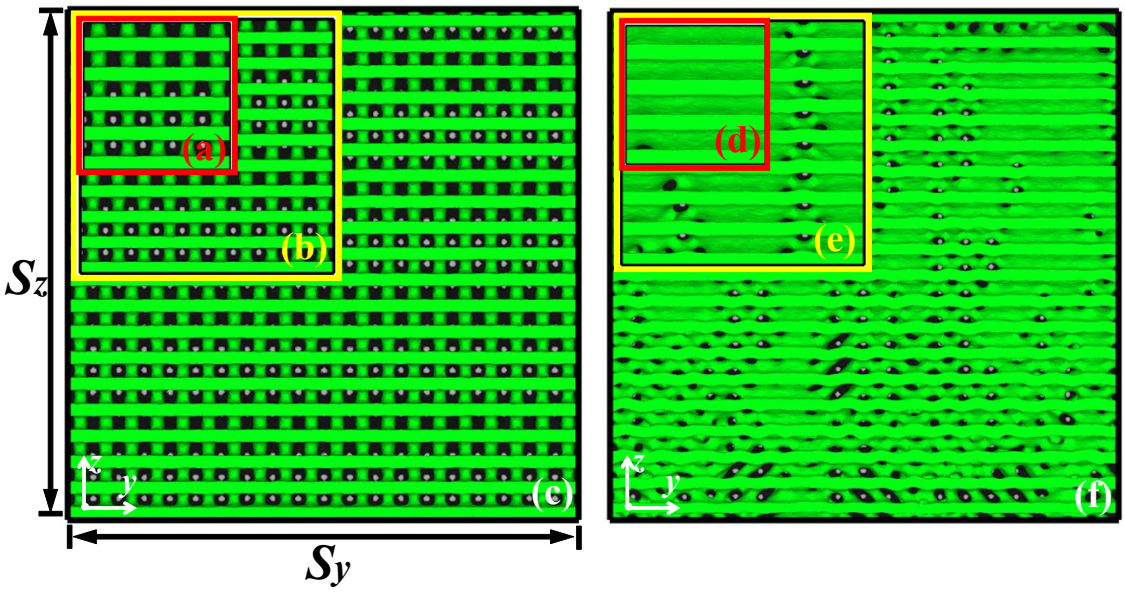

Fig. S1 Three-dimensional superstructures obtained from simulations with various box sizes in the cases of parameter settings of templates satisfied (a-c) commensurability conditions and (d-f) incommensurability conditions. The natural periodicity L_0 of lamellae is $3.6R_g$. In the cases of commensurability conditions, the stripe width is set as L_s=$3.6R_g$ and the periodicities of post arrays are set as L_y=$3.6R_g$ and L_z=$3.0R_g$. The box sizes H×S_y×S_z in the x, y and z directions are (a) $6.5R_g$×$18.0R_g$×$18.0R_g$, (b) $6.5R_g$×$36.0R_g$×$36.0R_g$, and (c) $6.5R_g$×$72.0R_g$×$72.0R_g$. In the cases of incommensurability conditions, the stripe width and the periodicities of post arrays are set as L_s=L_y=L_z=$4.45R_g$. The box sizes H×S_y×S_z in the x, y and z directions are (d) $6.5R_g$×$17.8R_g$×$17.8R_g$, (e) $6.5R_g$×$35.6R_g$×$35.6R_g$, and (f) $6.5R_g$×$89.0R_g$×$89.0R_g$.

Part B: Position Parameter Distributions of 3D Structures in Chemical Templates

To further verify the poorly controlled placements of grain interfaces in the chemical templates with film thickness H=6.5R_g, we also examine the influence of various parameters, such as the width W_s and the periodicity L_s of chemical stripes, and the interactions λN between the blocks and chemical stripes, on the positions of grain interfaces. As shown in Figure S2, the thick films of block copolymers maintain the histograms of position parameters at an approximately uniform distribution. The phenomena manifest the fact that the templates with two chemically patterned surfaces cannot effectively register the positions of grain interfaces inside the 3D ordered structures in the cases of thick films.

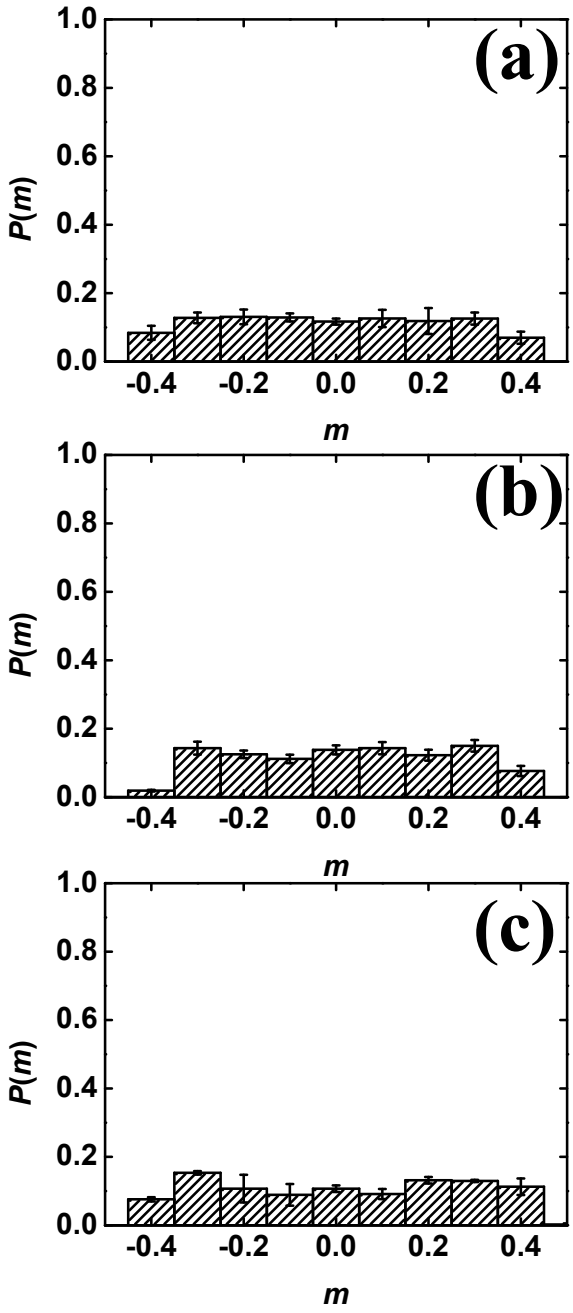

Fig. S2 Effects of design parameters of chemical stripes on probability distributions $P(m)$ of position parameters. The key parameters of chemical stripes are the same as those of Figure 2b except one parameter. (a) Interaction parameters $\lambda^t N$ and $\lambda^b N$ between the blocks and chemical stripes are changed from 10.0 to 5.0. (b) Periodicity L_s of chemical stripes is varied from $3.6R_g$ to $3.4R_g$. (c) Width W_s of chemical stripes is tuned from $1.8R_g$ to $1.6R_g$.

Part C: Free Energies of 3D Structures as a Function of Position Parameter

To understand the directed self-assembly behaviors of block copolymers in the chemical templates, the free energies of 3D structures with various averaged position parameters are calculated in the cases of film thickness H/R_g=4.0, 5.5 and 6.5. The difference Δ^H of free energy is defined as $H(\bar{m})$-$H(0)$, where $H(\bar{m})$ and $H(0)$ are the free energies of 3D structures at the averaged position parameters $\bar{m}$ and 0, respectively. As shown in Figure S3, the potential well is sharp at the film thickness H/R_g=4.0. The phenomenon manifests the fact that the grain interfaces are restricted to the center of thin films. However, the difference of free energies of 3D structures formed in the thick films (*e.g.*, H/R_g=5.5 and 6.5) is slight as the averaged position parameters are fluctuated in the range of $-0.30 \leq \bar{m} \leq 0.30$. This results in the observations of approximately uniform distribution of position parameters and the large standard deviations of averaged position parameters (Figures 2c and 2d).

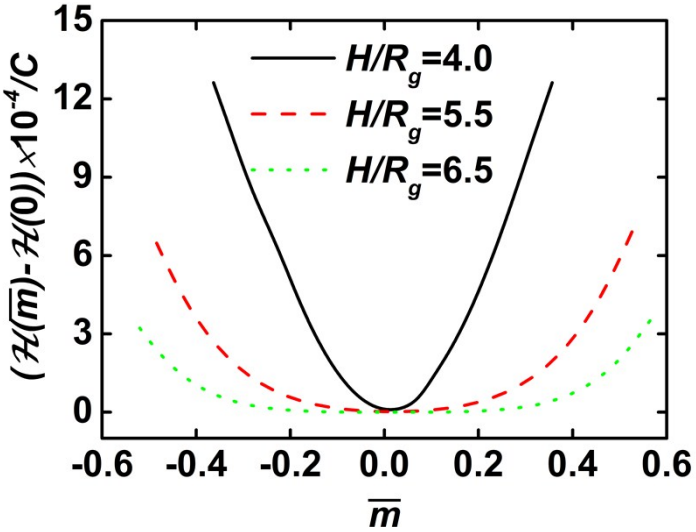

Fig. S3 Free energy density of three-dimensional structures as a function of averaged position parameter in the cases of film thickness H/R_g=4.0, 5.5 and 6.5. The difference ΔH of free energy is defined as $H(\bar{m})$-$H(0)$, where $H(\bar{m})$ and $H(0)$ are the free energies of three-dimensional structures at the averaged position parameters $\bar{m}$ and 0, respectively.

Part D: Self-Assembled Nanostructures Programmed by Topographical Posts

The topographical posts were originally introduced to direct the self-assembly of asymmetric block copolymers. The in-plane orientations and order degrees of cylindrical or spherical domains can be tailored by the commensurability conditions.[S6] To testify the above hypothesis for the in-plane orientations of lamellae perpendicular to the surfaces, we conduct the large-cell simulations of SCFT for the self-assembled structures of lamella-forming block copolymers directed by the post arrays with various periodicities. Similarly, the in-plane orientations of the vertical lamellae are also finely tuned by the periodicities of post arrays (Figure S4).

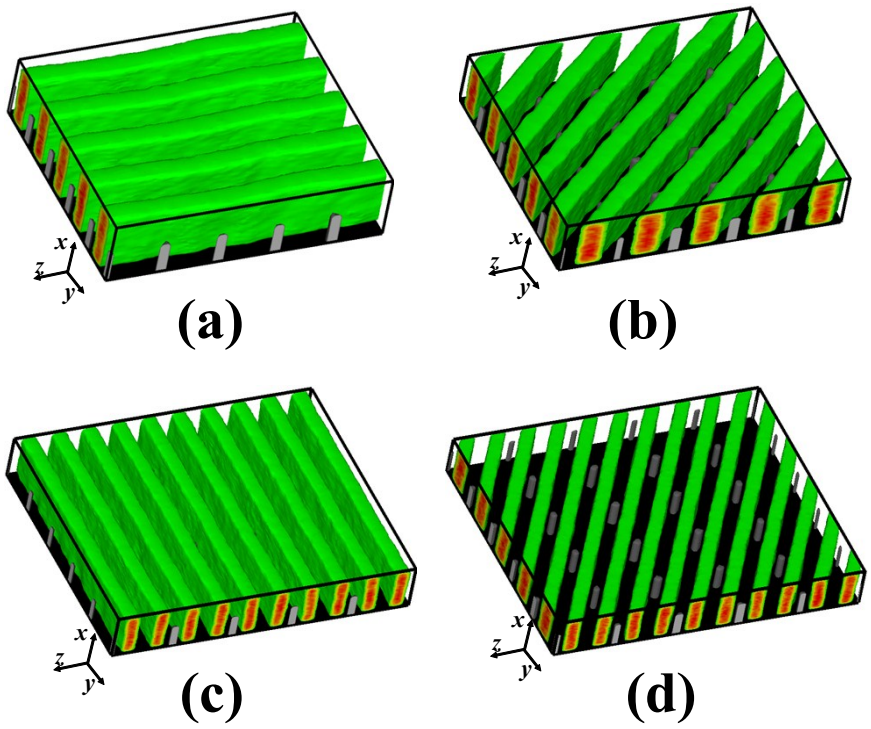

Fig. S4 Self-assembled nanostructures of symmetric block copolymers directed by post arrays with various periodicities. (a) L_y=4.0R_g and L_z=3.6R_g, (b) L_y=5.5R_g and L_z=4.6R_g, (c) L_y=7.2R_g and L_z=6.0R_g, and (d) L_y=8.4R_g and L_z=7.0R_g. Note that the top surfaces are assumed to be neutral.

Part E: Effects of Chemical Selectivities on Self-Assembled Structures

The chemical selectivities of the bottom surfaces show effects on the morphologies and orientations of self-assembled structures of block copolymers. Figures S5 and S6 display the self-assembly behaviors of block copolymers directed by the topographical templates and the hybrid templates with various chemical selectivities of bottom surfaces, respectively. An increase of the interactions between the B blocks and the bottom surfaces gives rise to the local change of self-assembled structures. When the bottom surfaces strongly repel the B blocks, A-rich flat layers are produced in the bottom part of films and destabilize the 3D ordered structures of vertical lamellae.

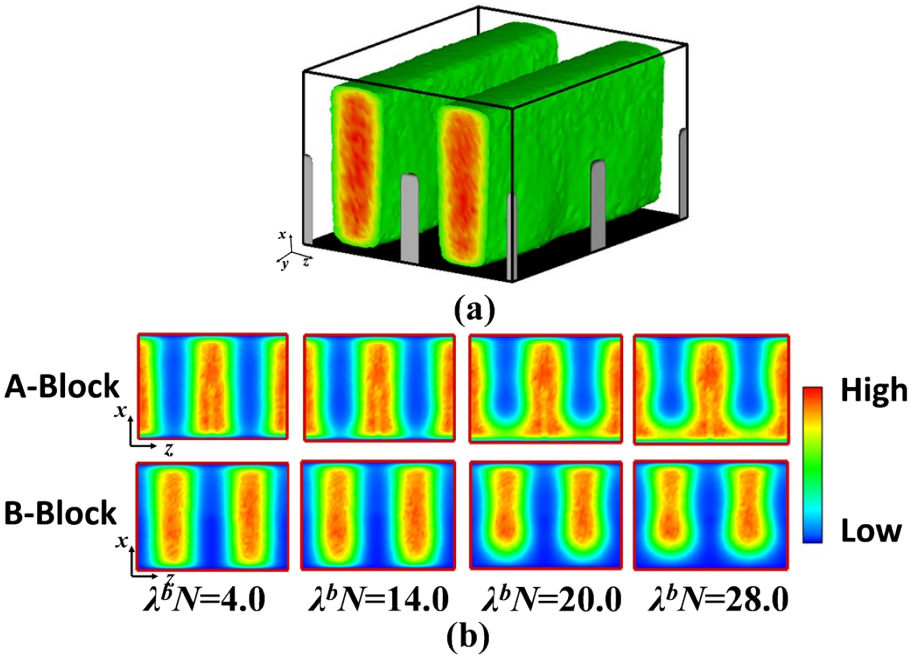

Fig. S5 Effects of interaction parameters $\lambda^b N$ between the bottom surfaces and the B blocks on morphologies of block copolymers guided by topographical posts. (a) Three-dimensional views of morphologies of block copolymers with interaction parameter $\lambda^b N$ =4.0. (b) Profiles of averaged volume fractions $\bar{\phi}_I(x,z)$ of A (top rows) and B (bottom rows) blocks in the *x*-*z* plane. The averaged volume fraction of *I*-type block is defined as $\bar{\phi}_I(x,z) = \frac{1}{N_y}\sum_{y=1}^{N_y} \phi_I(x,y,z)$. Note that the top surfaces are assumed to be neutral.

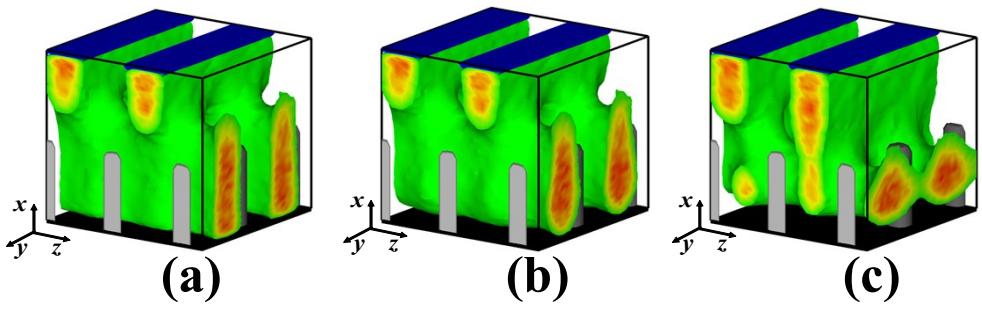

Fig. S6 Three-dimensional structures of block copolymers directed by hybrid templates for various interaction parameters between the B blocks and the bottom surfaces (a) $\lambda^b N$=0.0, (b) $\lambda^b N$=15.0 and (c) $\lambda^b N$=30.0.

Part F: Non-Orthogonally Crossed Structures Registered by Circular Posts

When the post arrays are very sparse, the block copolymers self-assemble into the poorly ordered architectures, where the lamellae with single in-plane orientation cannot completely fill the bottom part of films. As shown in Figure S7, the lamellae with degenerate orientations appear due to the isotropic characteristics of circular posts.

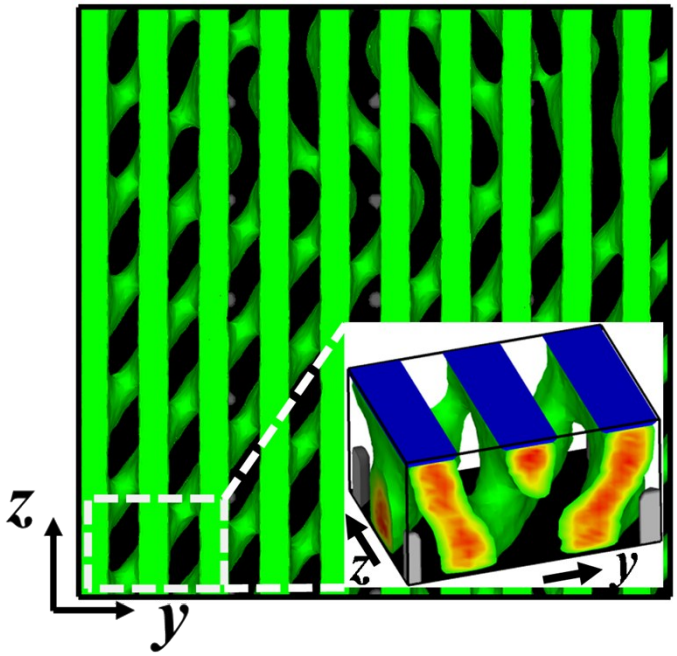

Fig. S7 Top-down views of non-orthogonally crossed structures of block copolymers guided by post arrays with periodicities L_y=9.0R_g and L_z=6.0R_g. Insets are the three-dimensional views of local structures enclosed in the dashed boxes. Note that the shape of posts is circular. Only 1/24 portion of the simulation cell is shown in the inset.

References

S1 G. H. Fredrickson, *The Equilibrium Theory of Inhomogeneous Polymers*; Oxford University Press, Oxford, 2006.

S2 L. Zhang, L. Wang and J. Lin, *ACS Macro Lett.,* 2014, **3**, 712.

S3 R. A. Mickiewicz, J. K. W. Yang, A. F. Hannon, Y.-S. Jung, A. Alexander-Katz, K. K. Berggren and C. A. Ross, *Macromolecules,* 2010, **43**, 8290.

S4 A. Ramírez-Hernández, G. Liu, P. F. Nealey and J. J. de Pablo, *Macromolecules,* 2012, **45**, 2588.

S5 S. Hur, A. L. Frischknecht, D. L. Huber and G. H. Fredrickson, *Soft Matter,* 2011, **7**, 8776.

S6 J. K.Yang, Y. S. Jung, J. B. Chang, R. A. Mickiewicz, A. Alexander-Katz, C. A. Ross and K. K. Berggren, *Nat. Nanotechnol.,* 2010, **5**, 256.

S7 M. Müller, *Phys. Rev. Lett.,* 2012, **109**, 087801.